Int. J. Electrochem. Sci., 15 **(2020)** 6522 – 6548, doi: 10.20964/2020.07.33

International Journal of
ELECTROCHEMICAL
SCIENCE
www.electrochemsci.org

Electrochemical Studies and the Electrode Reaction Mechanism of Ferrocene and Naphthoquinones in Microemulsion Medium at GC Electrode

M, Abdallah [1,2], Ahmed Alharbi[2], Moataz Morad [2], Ahmed M Hameed [2], Salih S. Al-Juaid [3], N. Foad [1] and E.M. Mabrouk[1]*

[1] Chem. Dept, Faculty of Science, Benha University, Benha, Egypt
[2] Chem. Dept., Faculty of Applied Sciences, Umm Al-Qura University, 21955 Makkah, Saudi Arabia
[3] Chem. Dept., Faculty of Science, King Abdulaziz University, Jeddah, Saudi Arabia
[*]E-mail: metwally555@yahoo.com

Received: 7 March 2020 / *Accepted:* 20 April 2020 / *Published:* 10 June 2020

The electrochemical behavior of 1,4-napthoquinone (1,4-NAQ) and 2-methyl-1,4-naphthoquinone (2-Me-1,4-NAQ) was investigated in bis-(2-ethylhexyl) sulfosuccinate (EHSS) anionic surfactant and its microemulsion system as well as in aqueous medium using cyclic voltammetry, rotating disk voltammetry and chronocoulometry techniques. The voltammograms of both compounds in all media exhibit a single redox couple and the ratios of I_{pa}/I_{pc} is slightly less than unity in all media. The $I_p - v^{1/2}$ plots gave linear correlations slightly deviated from the origin which denoting that the electrode reaction is mainly controlled by diffusion with slight adsorption contribution. For 1,4-NAQ and 2-methyl-1,4-NAQ in all media, the peak separation (ΔE_p), is not close to the theoretical value of completely reversible 2-electron transfer process (30 mV) which denotes that an ECE reaction nature and the reduction process of both compounds is quasi-reversible. This behavior is further confirmed by the cathodic shift of the rotating disk voltammograms as the angular velocity increases and the data of this technique were found in a good agreement with that obtained from cyclic voltammetry. The diffusion coefficient values of both compounds were calculated and the electrode reaction mechanism was suggested.

Keywords: Electrode reaction mechanism, CV, RDV and chronocoulometry techniques, naphthoquinones, GC electrode.

1. INTRODUCTION

Surfactants are molecules that possess hydrophilic and hydrophobic character. They may aggregate under favorable conditions in water to form microscopic domains called micelles [1]. At low concentrations in water, the surfactant molecules are simply dissolved. On increasing surfactant concentration, the solution conductivity increases and the surface tension decreases upon reaching a

certain concentration at which the surfactant molecules starts to aggregate, forming spherical objects called micelles [2]. The concentration at which the aggregation occurs is known as the critical micelle concentration (CMC). Above the CMC, further addition of monomer causes an increase in the number of micelles, thus the surface tension and conductance remain unchanged [2]. Electrochemistry is an important tool for studying micelles and microemulsions systems. Electrochemical techniques allows to measuring the diffusion coefficient of an electroactive substance in micelles and microemulsion systems. Electrochemical techniques that have used in such studies are polarography [3,4], cyclic voltammetry [5,6], rotating disk voltammetry [7-9] and chronoamperometry/chronocoulometry [9,10].

Quinoic compounds are of great importance to understood different processes that are related to biology. The quinone structure is common in numerous natural products that are associated with antitumor, antibacterial, antimalarial, antifungal as well as anticancer activities [11]. A series of natural and synthetic 2-hydroxy-3-methyl-alkylnaphthoquinone have relevant biological activities showed typical voltammogram on Hg and glassy carbon electrodes in aprotic medium (DMF-TBAP). Two main peaks, the first one corresponding to irreversible and second one to quasi-reversible process were observed (Reduction of biologically active 2-hydroxy-3-alkyl-1,4-naphthoquinone) [12]. The electrochemical reduction of 1,4-naphthoquinone derivatives was studied in DMS and acetonitrile in absence and presence of proton donors methanol and acetic acid and the effect of intermolecular hydrogen bonding on the electrochemical reduction of α-phenolic naphthoquinones was reported [13]. The electrochemical properties of substituted 2-methyl-1,4-naphthquinones were studied by cyclic voltammetry to build and evaluate a predictive structure-redox potential model. In aprotic solvent, 1,4-NQ reduction occurs through two successive one-electron transfers. Chronocoulometry/chronoamperometry were used to confirm that each successive reduction involve one electron transfer. The radical anion intermediate 1,4-NQ^{-} is formed in the first reduction step and is subsequently reduced to quinone dianions 1,4-NQ^{2-} in a second step [14]. The electrochemical behavior of anthraquinone (AQ) was studied in aqueous solution at glassy carbon electrode using cyclic voltammetry technique. A two-electron reduction transfer is obtained in aqueous solution. In micelles (CTAB/1-butanol/water) and microemulsion (CTAB/1-butanol/water/cyclohexane), the electrode reaction are nearly reversible at low oil (cyclohexane) content. At higher oil content, the reversibility is gradually lost [15]. Synthesis, structure and electrochemical properties of 2,5-bisaryl-1,4-benzoquinone and 2-arylamino-1,4-naphthoquinone were studied. These compounds showed a proton sensitive quasi-reversible cycle and the couple is affected by variation of the substituents on the nitrogen atom [16]. 1,2,3-triazole-arylamino and thio-substituted naphthoquinones were synthesized and evaluated against several human cancer and melanoma. The electrochemical properties of the synthesized compounds were investigated using cyclic voltammetry in an attempt to correlate them with antitumor activity [17].

In the last decay, electrochemistry of quinone compounds was the subject of several studies [18-20]. Little attention was paid to the electrochemical studies of naphthoquinones in microemulsion solutions. In continuation of our work for studying and suggestion of electrode reaction mechanism of organic compounds using polarography and cyclic voltammetry techniques in aqueous solution [21-23] and microemulsion systems [24], the present paper aimed to study the electrochemical behavior of 1,4-naphthoquinone and 2-methyl-1,4-naphthoquinone in aqueous and microemulsion solutions using cyclic

voltammetry to investigate the effect of composition of the medium on the electrochemical parameters and the electrode reaction mechanism.

2. EXPERIMENTAL

2.1. Materials

Bis (2-ethylhexyl) sulfosuccinate (EHSS) anionic surfactant was obtained from Aldrich chemicals. The hydrocarbon, n-decane was used as the oil and was obtained from Merck reagents. Sodium chloride (0.1M) and n-butanol were used as the electrolyte and the cosurfactant, respectively and were obtained from Sigma chemicals. All solutions were prepared using doubly distilled water.

2.2. Material micelle and microemulsion formulation

Micro-emulsions were formulated by subsequently adding surfactant (6% EHSS) hydrocarbon oil (3% n-decane), 4.5% courfactant (n-butanol) and finally water, however, changing the above sequence does not alter the phase behavior or the properties of the microemulsions. All components were weighed with accuracy of 0.2 ppm. After adding all components, the solutions were mixed with Vortex mixer for 30 min, heated up to 60 ^{o}C and then altrasonic for 30 min to make sure homogeneity of sample and one phase microemulsion was obtained. All samples were equilibrated in thermostated environmental room overnight at 22^{o}C. Equilibrium was considered to be achieved when the volume and microscopic structures observed did not vary with time under isothermal conditions. Micellar solutions were prepared in the same manner without adding hydrocarbon (oil) and cosurfactant (n-butanol).

1,4-naphthoquinone and 2-methyl-1,4-naphthoquinone were obtained from Fluka chemicals.

2.3. Materials purification

2.3.1. Ferrocene purification

Ferrocene was obtained from Fisher Scientific and was 98 % pure. Ferrocene was dissolved in absolute ethanol up to its saturation point, then recrystallized at 0 ^{o}C from ethanol for three or four times. Finally, the recrystallized ferrocene was sublimated in a battery dish to applying low and uniform heating to obtain ferrocene crystals.

2.4. Electrochemical experiments

2.4.1. Preparation of samples for electrolysis

The accurate amount of the electroactive probe (ferrocene, naphthoquinone derivatives) was added directly to a measured volume of microemulsion samples or micelles. The solution was stirred

and mixed in an altrasonic vibrator until all the solids dissolved. The sample was transferred to the electrochemical cell. Nitrogen gas was bubbled through the solution at a small rate (to avoid foaming of microemulsion) for about 10 min to remove all the dissolved oxygen. The temperature of the electrolysis solution was controlled at the desired temperature using thermostat water bath.

2.4.2. Instrumentation

The electrochemical experiments were performed using a computerized electrochemistry system model HQ-2030. The electrochemical analyzer interfaced with an IBM personal computer to store and further analysis. A glassy carbon (GC) electrode from BAS was used as the working electrode, a saturated calomel electrode was used as the reference electrode and platinum sheet of area 1 cm^2 was used as counter electrode. the working electrode was cleaned up by successive polishing with 5, 0.3 and 0.05 Um alumina on a piece cloth, then washed by distilled water, acetone and finally ultrasonicated in distilled water for about 15 min to retained aluminum oxide particles at the electrode surface. The area of the working electrode was estimated using cyclic voltammetry from two different reference systems:

1. 4mM $K_4Fe(CN)_6$ in 1M KCl, $D_o = 6.32x10^{-6}\ cm^2$ [25]
2. 4mM $K_3Fe(CN)_6$ in 1M KCl, $D_o = 7.63x10^{-6}\ cm^2$ [25]

From the known values of the diffusion coefficients for the two references systems, the area of the working electrode was determined to be 0.067 cm^2. All reference systems behaved reversibly.

The spectral studies were performed using Perkin Elmer spectrophotometer model JASCO V-330.

3. RESULTS AND DISCUSSION

3.1. Electrochemical characterization of EHSS micelle

To determine the critical micelles concentration (CMC) as well as solubilizes of EHSS micelles three different electrochemical techniques were used, cyclic voltammetry, rotating disk voltammetry and chronocoulometry.

3.1.1. Cyclic voltammetry (CV)

Cyclic voltammetry of $7x10^{-5}$ M of ferrocene as hydrophobic probe was recorded in anionic EHSS surfactant of different concentrations ranging between $1x10^{-4}$ to $2x10^{-3}$ M in 0.1M NaCl as a supporting electrolyte at different scan rates. The obtained voltammograms were recorded in potential window from 0.0 to 500 mV versus SCE at different sweep rates ranging from 20 to 500 mV/s. The voltammograms showed one anodic and one cathodic peak as represented in Fig. 1. The anodic peak current, I_{pa}, and the cathodic peak current, I_{pc}, are almost of equal heights and the ratio of i_{pa}/i_{pc} does not exceed 1.076 in solution of $2x10^{-3}$ M of EHSS, Table (1). Also, peak potential separation, $\Delta E_p = (E_{Pa} - E_{pc})$ is showed almost around the theoretical value for one-electron transfer (56-62 mV). The results indicate that the electrochemical oxidation of ferrocene (Fc) in EHSS micelles is a reversible 1-electron

transfer process forming ferrocenium ion as following:

$$Fc \leftrightarrow Fc^{+} + e \quad (1)$$

On using Randles-Sevcik equation [25]:

$$I_p = 0.4463\ (n^{3/2}\ F^{3/2})\ (R^{1/2}\ T^{1/2})\ D^{1/2}\ A\ C\ v^{1/2} \quad (2)$$

In which F is the Faraday constant (96487 coulombs), $D^{1/2}$ is the diffusion coefficient in cm/s^2, A is the electrode surface area in cm^2, C is the depolarizer concentration in m mol/L, v is the sweep rate in mV/s, R is the gas constant and n the total number of electrons involved in the electrode process. The plotting of I_p versus the square root of the scan rate, $v^{1/2}$, gives straight line intersecting the origin at all concentrations of EHSS (Fig. 2) which indicate that the electrode process is diffusion-controlled reaction [26-27].

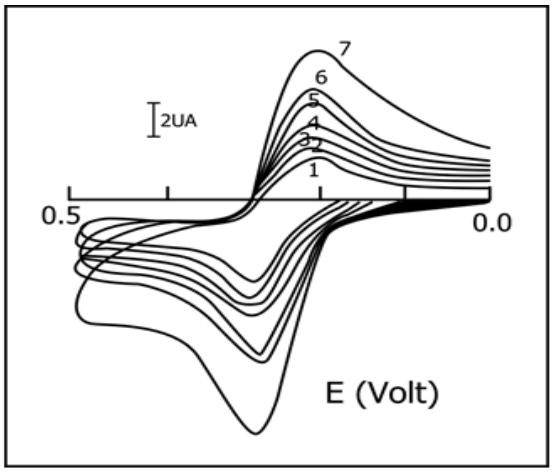

Figure 1. Cyclic voltammograms of $7x10^{-5}$ M ferrocene in $2x10^{3}$ M EHSS at different sweep rates, (1) 20, (2) 50, (3) 80, (4) 100, (5) 150, (6) 200, (7) 500 mV/s

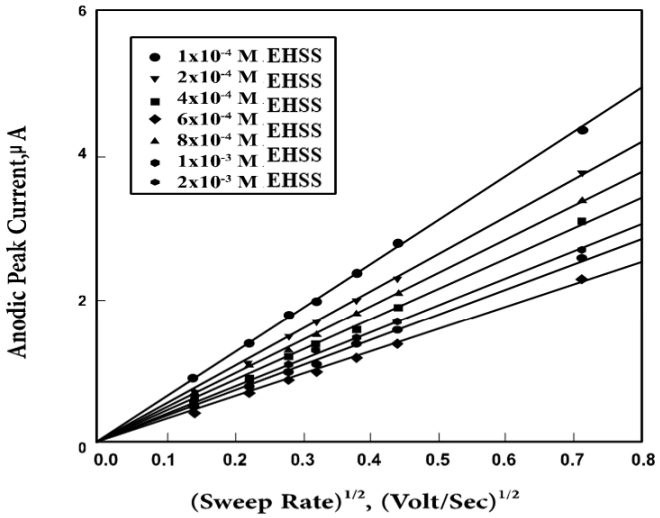

Figure 2. The plots of anodic peak current (I_{pa}) versus the square root of sweep rate ($v^{1/2}$) of $7x10^{-5}$ ferrocene in EHSS micellar solutions of different concentrations.

Also, the plot of I_{pa} versus surfactant concentration showed linear correlation consisting of two segments (Fig. 3A). The CMC of EHSS is determined at the point which break occurs. At CMC, the solution changes from surfactant solution (true solution) to aggregates (micelles}. The CMC was obtained at $5.05x10^{-4}$ M of EHSS in 0.1M NaCl at 25 ^{O}C. The CMC was further confirmed from the plots of E_{pa} versus surfactant concentration where the CMC of EHSS is defined as the point at which break occurs and may be attributed to structural changes (Fig. 3B).

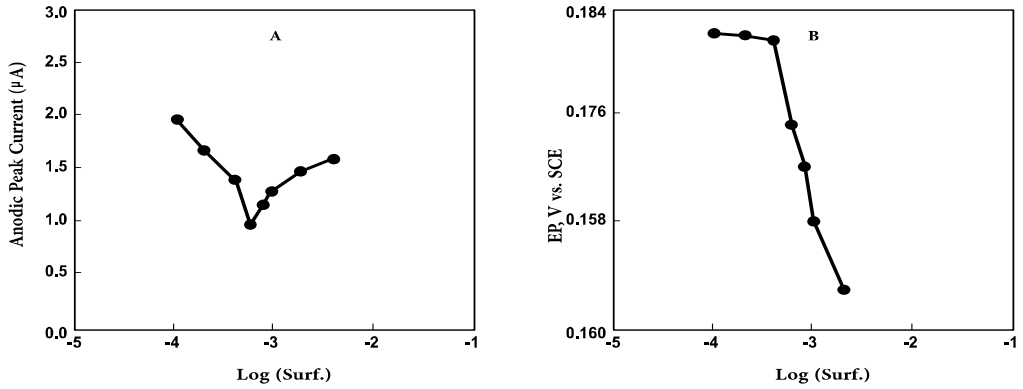

Figure 3. The plots of (a) anodic peak current, (b) anodic peak potential of $7x10^{-5}$ M ferrocene in EHSS micellar solutions at sweep rate 100mV/s versus the logarithm of surfactant concentration.

Table 1. Cyclic voltammetric data obtained for $7x10^{-5}$ M of ferrocene in EHSS micellar solutions of different concentrations.

concentration	Sweep rate, mV/ses	E_{pa} mV	E_{pc} mV	i_{pa} uA	i_{pc} uA	i_{pa}/i_{pc}	ΔE_p mV	$E_{1/2}$ mV
$1x10^{-4}$ M	20	180	121	1.30	1.29	1.007	59	150
	50	180	122	1.50	1.48	1.013	58	151
	100	182	123	1.80	1.80	1.000	59	152
	200	182	122	2.60	2.61	0.996	59	151
	500	183	121	4.08	4.07	1.001	62	152
$2x10^{-4}$ M	20	180	121	1.20	1.22	0.983	59	150
	50	180	122	1.40	1.41	0.992	58	151
	100	182	123	1.70	1.70	1.000	59	152
	200	181	122	2.50	2.51	0.996	59	151
	500	183	121	3.90	3.95	0.987	62	152
$4x10^{-4}$ M	20	180	121	1.22	1.21	1.008	59	150
	50	180	122	1.01	1.12	0.987	58	151
	100	182	121	1.46	1.43	1.020	59	150
	200	181	120	2.10	2.11	0.995	60	150
	500	183	122	3.40	3.42	0.994	59	151
$6x10^{-4}$ M	20	172	115	0.91	0.90	1.007	57	143
	50	173	116	1.04	1.03	1.013	57	133

	100	175	114	1.24	1.24	1.000	61	144
	200	176	117	1.74	1.80	0.996	59	146
	500	176	118	2.90	2.85	1.001	58	147
$8x10^{-4}$ M	20	170	112	0.74	071	1.042	58	141
	50	170	112	0.87	0.85	1.023	58	141
	100	172	114	1.10	1.11	0.990	58	143
	200	172	115	1.60	1.59	1.006	57	143
	500	173	116	2.60	2.57	1.011	57	144
$1x10^{-3}$ M	20	167	111	0.61	0.60	1.016	56	139
	50	167	110	0.72	0.71	1.014	57	138
	100	168	111	0.98	0.96	1.020	57	139
	200	169	113	1.40	1.38	1.014	56	141
	500	170	114	2.19	2.13	1.028	56	142
$2x10^{-1}$ M	20	162	106	0.43	0.42	1.023	56	134
	50	163	106	0.56	0.52	1.076	57	134
	100	163	105	0.94	0.90	1.040	58	134
	200	165	104	1.30	1.32	0.986	61	134
	500	166	108	2.01	1.99	1.030	58	137

3.1.2. Rotating disk electrode (RDE)

On using the RDE technique, a known concentration of the electroactive probe was added to a series of the monomeric surfactant solution, EHSS, containing 0.1M NaCl as a supporting electrolyte. The surfactant concentration was varied in the range $1x10^{-4}$ -$1x10^{-3}$ M. The effect of rotation speed on the voltammograms of $7x10^{-5}$ M electroactive ferrocene was recorded at rotation speed 250, 500, 750, 1000, 1250, 1500 and 2000 RPM (Fig. 4). The sweep rate used was 5 mV/s at all rotation speeds. The limiting current, i_L, measured from the current – potential response at the steady state was found to be linearly increased on increasing the rotation speed.

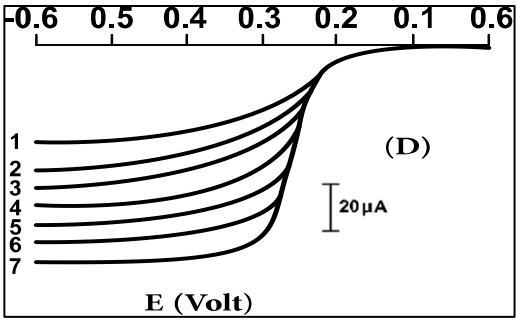

Figure 4. The effect of rotation speed of glassy carbon electrode on the linear sweep voltammograms obtained for $7x10^{-5}$ ferrocene in $1x10^{-3}$ M EHSS micellar solution, (1) 250, (2) 500, (3) 750, (4)1000, (5) 1250, (6) 1500, (7) 2000 rpm.

On the other hand, the i_L, is decreased on increasing the surfactant concentration up to $6x10^{-6}$ M followed by sharp decrease. This decrease in I_L is not attributed to surfactant adsorption because

chronocoulometry showed that there is a negligible adsorption at all surfactant concentration. Therefore, this decrease can be only attributed to structural changes of surfactant and a transition from true surfactant solution to aggregates (micelles) occurs.

On applying Levich equation [28]:

$$I_L = 0.62\ n\ FA\ C\ D^{2/3}\ v^{-1/6}\ \omega^{1/2} \quad (3)$$

in which ω is the angular velocity, rad s^{-1}, and the other terms have their usual significances. The plot of I_L versus $\omega^{1/2}$ for the electrochemical oxidation of ferrocene at different EHSS concentrations gives linear correlations passing through the origin (Fig. 5), confirming the diffusion nature of the electrochemical oxidation reaction. On the other hand, on increasing the rotation speed (ω), the half-wave potential ($E_{1/2}$) of the rotating disk voltammograms was held constant revealing the reversibility of the ferrocene oxidation process. Furthermore, on using the following equation [27]:

$$E = E_{1/2} - RT/nF \ln i/(i_L - i) \quad (4)$$

and on plotting log $i/(i_L - i)$ versus E (not shown) at rotation speed 1000 rpm, applying the logarithmic analysis of the rotating disk voltammograms, a straight line of slope amounting to 0.053 is obtained, which corresponding to a one electron transfer process.

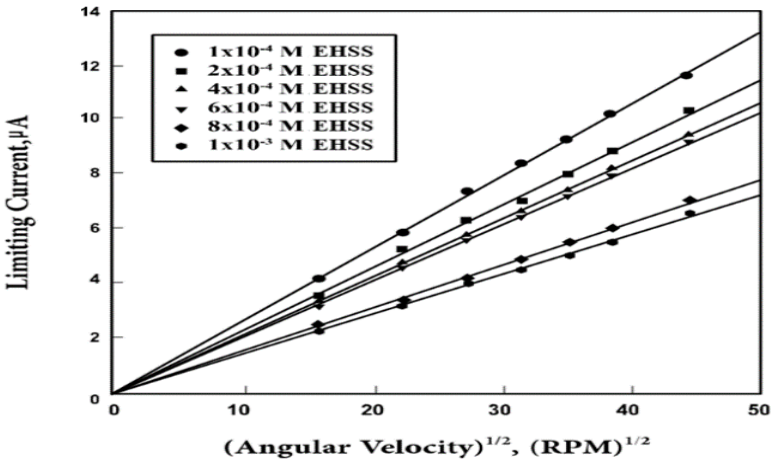

Figure 5. The plots of the limiting current (I_L) versus the square root of angular velocity ($\omega^{1/2}$) for $7x10^{-5}$ ferrocene in different concentrations EHSS micellar solution

3.1.3. Solubility of ferrocene in EHSS

The rotating disk voltammetry was used to determine the diffusion coefficient of EHSS micelles in 0.1M NaCl solution, in the range from $6x10^{-4}$ to $1x10^{-2}$ M of surfactant, by using ferrocene as the hydrophobic electroactive probe. The concentrations of ferrocene were very close to the saturation concentration in each micellar solution. The amounts of ferrocene solubilized in EHSS micelles were determined using spectrophotometric technique in the UV-visible range. The absorbance values measured at wavelength 440 nm for ferrocene solubilized at different surfactant concentrations were compared with the calibration graph (not shown) of ferrocene in pure ethanol and listed in Table 2. Under these conditions, ferrocene was also present in the aqueous phase and was assumed to be soluble in the electrolyte 0.1M NaCl. The diffusion coefficient values obtained directly from the slopes of the straight

lines obtained on plotting I_L versus $\omega^{1/2}$ using Levich equation represent the apparent diffusion coefficient values (D_a). These apparent diffusion coefficients of ferrocene are the sum of diffusion coefficients of ferrocene in in the aqueous phase and that present in micelle. So correction was made to obtain a better estimation of the actual micelle diffusion coefficient by knowing the relative concentrations of probe in the aqueous phase and in the micelle. The redox behavior of ferrocene as the hydrophobic probe was treated depending on the exit-entrance rate using two methods of treatment, slow rate which termed as zero-kinetics and fast rate (fast-kinetics approximation).

Table 2. Diffusion coefficient values of solubilized ferrocene in EHSS micellar solutions obtained from RDV measurements.

[Surfactan] (mM)	**[Ferrocene] (M)**	**D_a (10^{-6} cm^2 s^{-1})**	**D_d (10^{-6} cm^2 s^{-1})**	
			Slow[a]	**Fast[b]**
0.6	$5.25x10^{-4}$	1.985	1.892	2.350
0.8	$6.00x10^{-4}$	1.103	0.962	1.440
1.0	$7.07x10^{-3}$	0.715	0.558	0.992
2.0	$8.86x10^{-4}$	0.409	0.245	0.617
4.0	$1.13x10^{-4}$	0.208	0.052	0.346
10.0	$2.50x10^{-3}$	0.077	0.010	0.139

D_a is the apparent diffusion coefficient in aqueous media, D_d is the corrected micellar diffusion coefficient.

a: calculated in zero-kinetic (slow) approximation. b: calculated in fast-kinetic limit.

3.2. Electrochemical characterization of EHSS microemulsion system

3.2.1. Cyclic voltammetry (CV)

The voltammograms of 1mM ferrocene were recorded in EHSS microemulsion containing 6% EHSS as the surfactant, 3% n-decane as the oil and 4% n-butanol as the cosurfactant in 0.1M NaCl supporting electrolyte. The voltammograms were recorded in the potential window from 0.0 to + 500 mV (versus SCE) and at potential sweep rate 20-500 mV/sec. Well-defined voltammograms were obtained showing one anodic and one cathodic peak (Fig. 6). The anodic peak current, i_{pa}, and the cathodic peak current, i_{pc}, are almost of equal heights (Table 3). The anodic to cathodic peak current ratios (i_{pa}/i_{pc}) does not exceed 1.095 9 (Table 3), (which indicate the reversibility of the electrode process and confirmed that there is no adsorption contribution to the electrode surface. Moreover, the peak potential separation ($\Delta E_p = E_{pa} - E_{pc}$) is around the theoretical value for one-electron transfer (56-60

mV) in EHSS microemulsion system (Table 3). These results indicate that, the electrochemical oxidation of ferrocene is one-electron transfer process.

The fully reversible one-electron diffusion-controlled step representing the redox process of ferrocene to the ferrocenium ion in EHSS micellar and EHSS microemulion which is defined by equation (1) was supported by several studies included the oxidation of simple ferrocene and ferrocene substituted compounds in different media using cyclic voltammetry technique. Neghmouche et al.,[29] studied the oxidation of simple ferrocene in dichloroethane solvent and aqueous ethanol in tetrabutylammonium tetraflouroborate Bu_4NBF_4 as a supporting electrolyte. The cyclic voltammograms displayed a fast one-electron transfer step. The i_{pa} / i_{pc} ratio is close to one and the plots of i_{pa} and i_{pc} versus the square root of the scan rate $v^{1/2}$ gave linear correlation pass through the origin–indicating the reversibility and the diffusion redox process [29]. Also, Tsierkesos examined the oxidation of simple ferrocene in different solvents, ACN, NME, DMF, DMA, DMSO and DCM using cyclic voltammetry technique. A single one-electron reversible oxidation wave was observed. The diffusion coefficient values of ferrocene have been calculated using Randles-Sevcik equation. The effect of changing scan rate and solvent properties was also examined [30]. The oxidation of simple ferrocene in propylene carbonate solvent and $LiClO_4$ as supporting electrolyte was investigated using cyclic voltammetry technique. The results indicated that the redox process occurs through a single one-electron quasi-reversible diffusion controlled step [31]. The electrochemical behavior of a series of 2,7-substituted-9-fluoronl-ferrocene [32] and the benzyl-substituted ferrocene [33] have been studied using cyclic voltammetry technique. All of these derivatives undergo a chemically reversible diffusion-controlled one-electron step at almost coincident potential values. The oxidation of the latter benzyl-substituted ferrocene compounds is more easily than ferrocene itself. The comparison between our results of ferrocene oxidation, which indicated a single fully reversible one-electron diffusion-controlled process and the results of oxidation of similar simple ferrocene or ferrocene substituted compounds [34,35], illustrates the congruence of our study and the other similar ones in literature. This conception indicates that our proposal of mechanistic ferrocene oxidation pathway is acceptable.

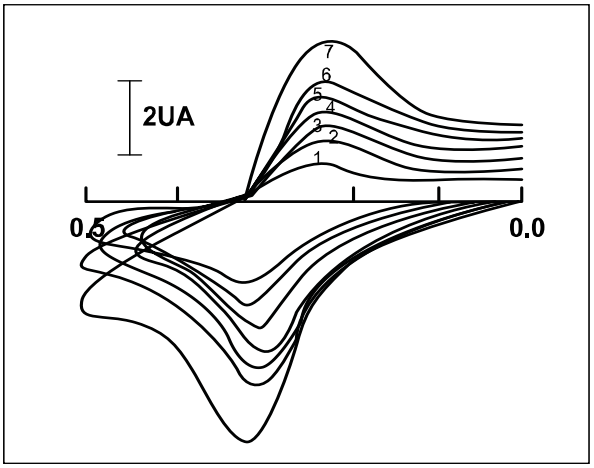

Figure 6. Cyclic voltammograms of $1x10^{-3}$ M ferrocene recorded in EHSS microemulsion system.

Applying Randless-Sevcik equation and on plotting the anodic peak current, $i_{pa,}$ versus the square root of sweep potential, $v^{1/2}$, at different concentrations of ferrocene straight lines intersecting the origin were obtained (similar that as shown in Figure 2), indicating that the electrode reaction is diffusion controlled [27]. The slopes of these plots were used to estimate the apparent diffusion coefficient of ferrocene in EHSS microemulsion and listed in Table (6). Ferrocene (Fc) is hydrophobic in nature, its solubility in water is $5x10^{-5}$ M [34] and of solubility 0.15 M in dodecane [35]. On the other hand, singly charged Fc^+ cation is water soluble, thus $Fc^{0/+}$ couple represents the limiting case where one form of the probe is oil soluble (Fc) and the other (Fc^+) is water soluble. By using Stock-Einstein equation, the values of the apparent diffusion coefficients of microemulsion were determined and thus, the radius of microemulsion droplets can be estimated and listed in Table (4).

Table 3. Cyclic voltammetric data obtained for different concentrations of ferrocene in EHSS microemulsion system.

concentration	Sweep rate, mV/ses	E_{pa} mV	E_{pc} mV	i_{pa} uA	i_{pa} uA	i_{pa}/i_{pc}	ΔE_p mV	$E_{1/2}$ mV
$2x10^{-4}$ M	20	233	176	0.54	0.56	0.960	57	204
	50	233	176	0.88	0.91	0.967	57	204
	100	235	177	1.20	1.30	0.923	58	206
	200	237	176	1.80	1.90	0.947	61	206
	500	244	175	2.70	2.90	0.931	61	205
$4x10^{-4}$ M	20	273	181	0.79	0.80	0.989	56	209
	50	238	180	1.20	1.30	0.923	58	209
	100	239	180	1.90	1.80	1.055	59	209
	200	241	184	2.50	2.512.6	0.961	57	212
	500	242	183	3.80	3.90	0.923	59	212
$8x10^{-4}$ M	20	238	181	0.98	1.02	0.960	57	209
	50	238	181	1.40	1.40	1.000	57	209
	100	240	182	2.08	2.10	0.990	58	211
	200	242	183	2.97	3.10	0.958	59	212
	500	244	185	4.87	4.80	1.014	59	214
$1x10^{-3}$ M	20	232	175	1.05	1.02	1.029	58	203
	50	233	177	1.60	1.85	0.864	56	205
	100	235	177	2.40	2.30	1.043	58	206
	200	238	179	3.30	2.90	0.916	59	208
	500	239	180	5.60	3.60	0.946	59	209
$2x10^{-3}$ M	20	245	185	1.30	1.30	1.000	60	215
	50	246	186	2.10	2.07	1.014	60	216
	100	248	190	2.96	2.99	0.989	58	219
	200	251	192	4.10	4.30	0.953	59	221
	500	252	193	6.70	6.80	0.985	59	222
$3x10^{-3}$ M	20	247	189	1.60	1.70	0.941	58	218
	50	248	190	2.40	2.50	0.960	58	219
	100	251	191	3.50	3.60	0.972	60	221
	200	254	195	4.70	4.90	0.959	59	225
	500	255	197	7.90	8.10	0.975	58	226

Table 4. Diffusion coefficient and the radius of microemulsion droplets in microemulsion system containing 6% EHSS, 3% n-decane, 4.5% n-butanol at different concentrations of ferrocene using CV measurements.

[Ferrocene] mM	**D_a x 10^{-7} R_h** **cm^2/s**	**A^o**
0.2	11.7	21
0.4	5.56	44
0.8	2.13	115
1.0	1.85	133
2.0	1.30	188
3.0	0.94	260

3.2.1.1. Effect probe concentration

The voltammograms obtained at different concentrations of ferrocene in the range $2x10^{-4} – 3x10^{-3}$ M (not shown) indicate an increase in peak current as the concentration of the probe increases in microemulsion system. The ratio of i_{pa}/i_{pc} within this concentration of the probe does not exceed 1.043 at different sweep rates. Also, peak potential separation, ΔE_p, is showed almost around the theoretical value for one-electron transfer. The results indicate that the electrochemical oxidation of ferrocene (Fc) in EHSS microemulsion is a reversible 1-electron transfer process forming ferrocenium ion as given in equation (1). On the other hand, the values of the half-wave potential of the voltammograms within the studied range of concentration was constant which ascertains the reversible nature of the electrochemical process.

3.2.1.2. Effect of hydrocarbon content

The effect hydrocarbon (oil) content on the diffusion coefficient and the radius of microemulsion system of EHSS was studied in the range from 2.0 to 3.5% (wt/wt) of n-decane using ferrocene as electroactive probe. Cyclic voltammograms obtained at different percentages of oil content and different sweep rates indicate a slight decrease in peak current on increasing the oil content. The anodic to cathodic peak current ratios (i_{pa}/i_{pc}) does not exceed 1.018 which indicates the reversibility of the electrode process and confirmed also that there is no adsorption contribution to the electrode surface. Results obtained showed also that as the oil content increases, the heterogeneity of the microemulsion system increases and this reflects the increased size of the droplets.

3.2.1.3. Effect of surfactant concentration

The effect surfactant concentration on the diffusion coefficient of AQT microemulsion was checked by using cyclic voltammetry. The surfactant concentration was varied in the range 5.0 - 6.5% (wt/wt). The other components of microemulsion system were held constant. The recorded voltammograms of 1 mM of ferrocene at different percentages surfactant (not shown) indicated that the I_p increases on increasing surfactant concentration in the microemulsion system. The plot of I_p versus $v^{1/2}$ gives straight lines passing through the origin (not shown), revealing the diffusion-controlled behavior of the electrochemical oxidation process. From the slopes of these plots, the diffusion coefficient values were calculated and showing an increase in their values as the surfactant concentration is increased (Table 5).

Table 5. Diffusion coefficient and the radius of microemulsion droplets of 1 mM ferrocene in microemulsion system containing, 3% n-decane, 4.5% n-butanol at different concentrations of EHSS surfactant using CV measurements.

% EHSS	**D_o x10^{-7} cm^2/ sec**	**R_b. A^o**
5.0	1.14	215
5.5	1.36	181
6.0	1.85	113
6.5	2.43	101

3.2.2. Rotating disk voltammetry (RDV)

The rotating disk voltammetry experiments were carried out successfully in EHSS microemulsion system in the range from $2x10^{-4}$ - $3x10^{-3}$ M of ferrocene electroactive probe. The microemulsion composition was held constant at 6% EHSS as the surfactant, 3% n-decane as the oil, 4.5% n-butanol as the cosurfactant containing 0.1M NaCl. The effect of rotational speed at angular velocity from 250 to 2000 RPM of the glassy carbon electrode was carried out using liner sweep voltammetry. The voltammograms were recorded at small sweep rate (5 mV/s) to obtain a steady state plateau and to avoid peaked shaped. The voltammograms in EHSS microemulsion system show one step oxidation-plateau (Fig. 7). The voltammogram revealing that, the limiting current (i_L) increases as the angular velocity (w) is increased, whereas the ($E_{1/2}$) is constant and not affected by the electrode rotation. The constancy of the $E_{1/2}$ revealed the reversibility of ferrocene oxidation in this medium.

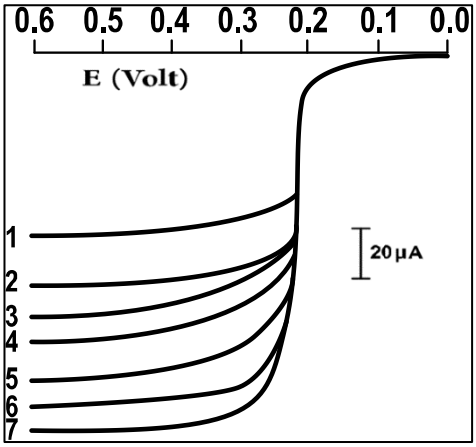

Figure 7. The effect of rotation speed of glassy carbon electrode on the linear sweep voltammograms obtained for $7x10^{-5}$ ferrocene in $1x1^{3}$ M EHSS micellar solution, (1) 250, (2) 500, (3) 750, (4)1000, (5) 1250, (6) 1500, (7) 2000 rpm.

Applying the Levich equation and on plotting i_l versus square root of the angular velocity ($\omega^{1/2}$), linear correlation passing through the origin were obtained (similar that as shown in Figure 5). The limiting current values were measured at the steady state at 400 mV. These typical results indicated that the electrode process is under mass transfer control. The slopes of the linear plots were used to estimate the apparent diffusion coefficients of microemulsion droplets by using Levich equation. Generally, a good agreement for the diffusion coefficient values obtained from rotating disk voltammetry and those obtained from cyclic voltammetry (Table 6).

Table 6. Diffusion coefficient and the radius of microemulsion droplets in microemulsion system containingg 6% EHSS, 3% n-decane, 4.5% n-butanol at different concentrations of ferrocene using RDV measurements.

[Ferrocene] mM	**$D_a x10^{-7}$**	**R_h**
	cm^2/s	**A^o**
0.2	10.50	23
0.4	5.36	34
0.8	2.02	114
1.0	1.71	130
2.0	1.42	172
3.0	1.01	242

3.2.3. Chronocoulometry (CC)

Choronocoulometry is an extremely valuable technique for the direct measurement of adsorption of electroactive species. Double potential step used to get information about the adsorption in the electrochemical system. The chronocoulometric response of ferrocene in EHSS micelles and microemulsion systems were recorded by plotting the charge versus time after taking the cyclic voltammograms in the same potential window. The stepping time was 250 ms and the potential widow was from 0.0 to 500 mV, which pre-selected from cyclic voltammetric behavior of ferrocene recorded in both EHSS micelles and microemulsion. Typical chronocoulograms of the forward step in these systems were obtained on plotting the total amount of diffusional charge, Q_{tot}, versus time, t, as represented in Fig. (8). Also, the Anson plots were tested by plotting the charge, Q_{tot}, versus $t^{1/2}$ and Q_r versus $\theta^{1/2}$ for the forward and reverse steps by using the following two equations [36,37]:

$$Q_{tot} = [2nFAD_o^{1/2} C_o t^{1/2}] / \pi^{1/2} + Q_c + Q_{ads} \quad (5)$$

$$Q_r = [2nFAD_o^{1/2} C_o \theta^{1/2}] / \pi^{1/2} + Q_c + nFA\Gamma^o \quad (6)$$

where $Q_{ads} = nFA\Gamma^o$

From the difference of intercepts of the forward and reverse steps of the Anson plots, the capacitive component in Q_{tot} is cancelled out. The amount of adsorbed reactant species (Γ^o) can be obtained quantitatively in general from the relation:

$$\text{Intercept 1} - \text{Intercept 2} = nF(\Gamma^o - \Gamma_r) \quad (7)$$

The calculated values of Γ^o ferrocene in EHSS micelles and EHSS microemulsion systems is in the range of 10^{-12} to 10^{-13} moles, indicating a negligible surfactant adsorption at the electrode surface.

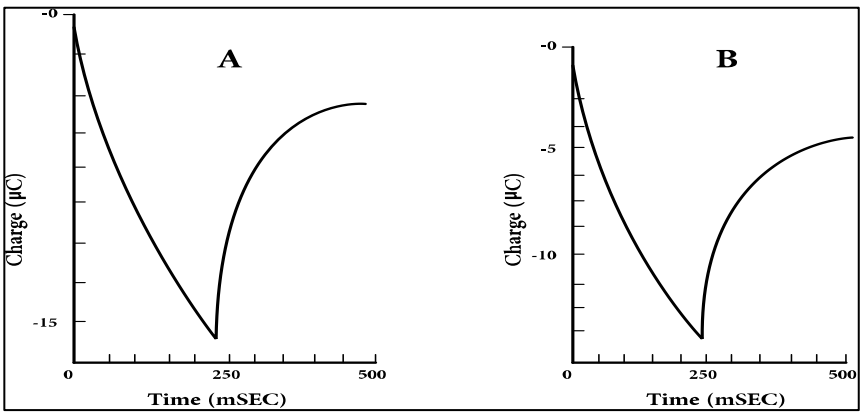

Figure 8. Chroncoulometric response of 1 mM ferrocene in (A) EHSS micelle and (B) EHSS microemulsion system.

3.3. Electrochemical investigation of 1,4-Naphthoquinone (NQ) in micelles and microemulsion media

3.3.1. Cyclic voltammetry measurements

The cyclic voltammograms of 1 mM of NQ in presence of 0.1 M NaCl as supporting electrolyte at different scan rates (20 – 500 mV/s) were recorded in EHSS micelles and microemulsion systems as

well as in pure aqueous solution, it is poorly soluble in water ($6x10^{-4}$ M). Its solubility is greatly enhanced by EHSS micelles and EHSS micoemulsion. The voltammograms displayed one cathodic peak in the cathodic scan and one anodic peak in the reverse scan (Fig.9A,B,C). The voltammograms in pure aqueous solution showed a similar voltammetry response, a single redox peak (Fig. 9A). The peak potential, ΔE_p, for aqueous solution is around 40 mV, whereas in EHSS micelles and EHSS microemulsion are around 107 and 92 mV, respectively (Table 7).

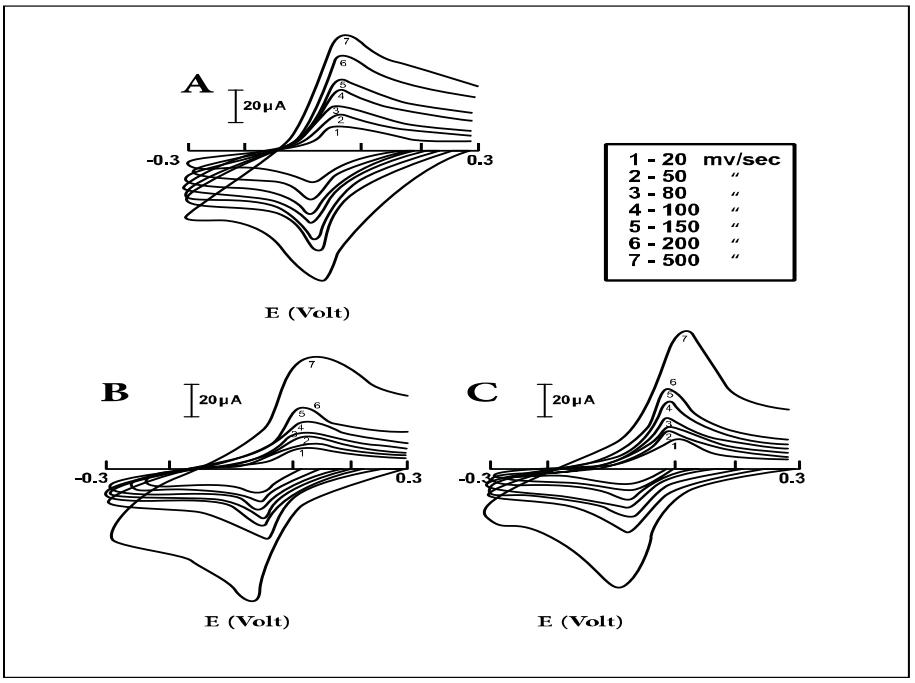

Figure 9. Cyclic voltammograms of $1x10^{-3}$ M 1,4-naphthoquinone recorded in A) Aqueous solution, B) EHSS micelle solution, C) EHSS microemulsion system

Table 7. Cyclic voltammetry data obtained for 1mM of 1,4-naphthoquinone in different systems.

Concentration	**Sweep rate, mV/ses**	**E_{pa} mV**	**E_{pc} mV**	**i_{pa} uA**	**i_{pa} uA**	**i_{pa}/i_{pc}**	**ΔE_p mV**
Pure aqueous	20	381	341	5.69	7.12	0.799	40
	50	382	341	12.60	14.30	0.881	41
	100	383	343	21.34	23.01	0.927	40
	200	384	344	30.04	31.99	0.939	40
	500	386	345	52.30	54.30	0.963	41
EHSS micelles	20	300	408	6.87	10.50	0.654	108
	50	301	408	11.87	17.50	0.678	107
	100	302	410	18.50	27.60	0.670	108

	200	304	410	25.90	39.89	0.649	106
	500	306	412	44.40	65.98	0.672	106
EHSS microemulsionn	20	362	452	15.30	19.60	0.921	90
	50	362	452	24.70	30.20	0.817	90
	100	364	455	38.00	45.00	0.844	91
	200	363	457	52.30	60.85	0.859	94
	500	364	458	84.90	98.90	0.858	94

The data listed in Table (7) revealed that in EHSS microemulsion system, the ΔE_p increases slightly from 90 to 94 mV as the scan rate increases. Since the peak potential separation, ΔE_p, in completely reversible systems is equal to 59 mV for 1-electron transfer process and equals close to 30 mV for reversible 2-elcetron process and in the present study it is around 40, 107 and 90 mV in aqueous, EHSS micelles and EHSS microemulsion solutions, respectively (Table 7), thus, it is concluded that an electrochemical-chemical-electrochemical (ECE) reaction occurs in these media in which protonation of the anion free radical generally leads to disprotonation reaction [38,39]. On the other hand, the ratio of I_{pa}/ I_{pc} at higher scan rates is slightly less than unity in aqueous and EHSS microemulsion but this ratio decreases to be between 0.65 and 0.68 in EHSS micelles (Table 7).

On employing the Randles-Sevcik equation, the plots of the anodic peak current, I_{pa}, and cathodic peak current, I_{pc}, versus the square root of sweep rate, $v^{1/2}$, in the different solutions, linear correlations deviated from the origin are shown (Fig,10). From the slopes of these plots, the apparent diffusion coefficient values of the oxidized and reduced species, D^o_O and $D^o_{R,}$ were calculated and found equal to $7.04x10^{-6}$, $1.7x10^{-6}$ and 7. $5.76x10^{-6}$ for D^o_O and $7.19x10^{-6}$, $3.36x10^{-6}$ and $7.46x10^{-6}$ cm^2/s for D^o_R in aqueous, EHSS micelles and EHSS microemulsion, respectively.

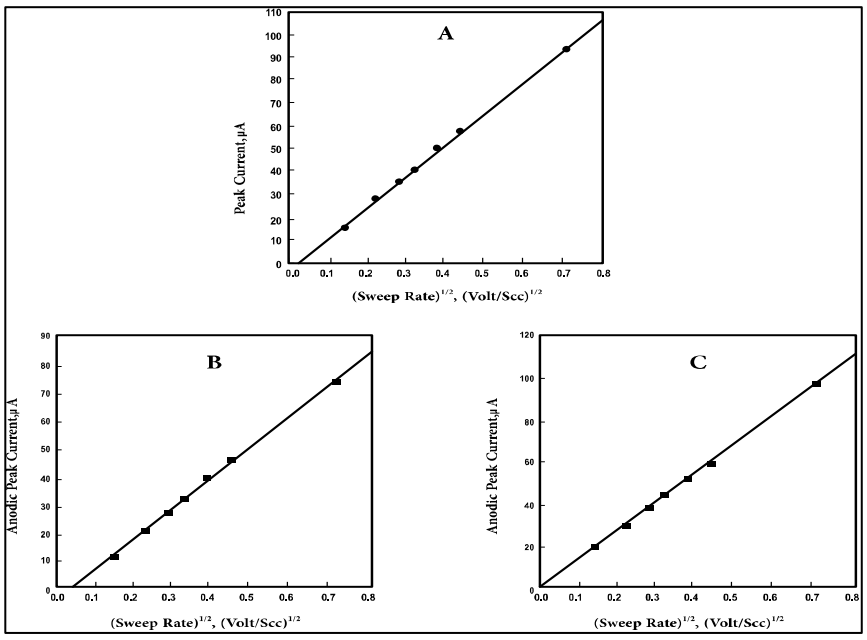

Figure 10. The plots of cathodic peak current (I_{pc}) versus the square root of sweep rate ($v^{1/2}$) in different media: A) Aqueous solution, B) EHSS micellar solution, C) EHSS microemulsion system.

3.3.2. Rotating disk voltammetry

The rotating disk voltammograms (RDV) of 1 mM of 1,4-naphthquinone were recorded at small sweep rate (5 mV/s) in the potential window 800 to 1000 mV in pure aqueous solution as well as in EHSS micelles and EHSS microemulsion systems. The RDVs displayed single reduction wave in all media (Fig.11).

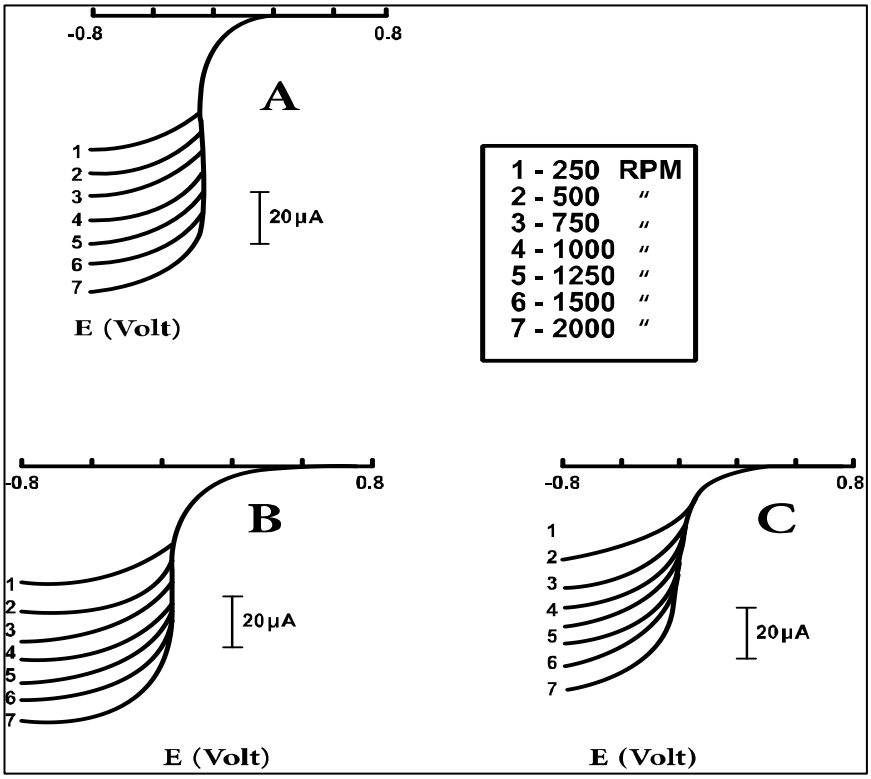

Figure 11. The effect of rotation speed of glassy carbon electrode on the linear sweep voltammograms obtained for 1mM in 1.4-naphthoquinone, (1) 250, (2) 500, (3) 750, (4)1000, (5)1250, (6)1500, (7)2000 rpm, A) Aqueoussolution, B) EHSS micellar, C)EHSS microemulsion.

It was found that, on increasing the rotation from 250 to 2000 RPM, a negative shift (~ 20mV) in the half-wave potential, $E_{1/2}$, indicating the chemical irreversibility which coincides with the greater ΔE_p values obtained from CV measurements. Logarithmic analysis of the RDVs were performed on plotting of log $(i/i_{L-} i)$ versus E in all investigated solutions which displayed parallel linear correlations at different rotation speed (250, 1000 & 2000 RPM) of slopes amounting to 10.7, 5.8 and 10.7 V for aqueous, EHSS micelles and EHSS microemulsion systems, respectively. These results indicate the quasi-reversible electron transfer process, since the calculated transfer coefficients (α) of the electro-reduction process in the aqueous, EHSS micelles and EHSS microemulsion systems are 0.64, 0.35 and 0.64, respectively.

On using Levich equation, the plots of I_L versus in all media showed linear correlations passing through the origin (Fig.12), the behavior which indicates that the reduction process of NQ takes place

under mass transfer control. From the slopes of these plots, the apparent diffusion coefficient values were calculated and found equal to $7.17x10^{-6}$, $2.76x10^{-6}$ and $6.05x10^{-6}$ cm^2/s in aqueous, EHSS micelles and EHSS microemulsion, respectively. The obtained results indicated the agreement of the D^o_R values calculated from cyclic voltammetry and those calculated from rotating disk voltammetry.

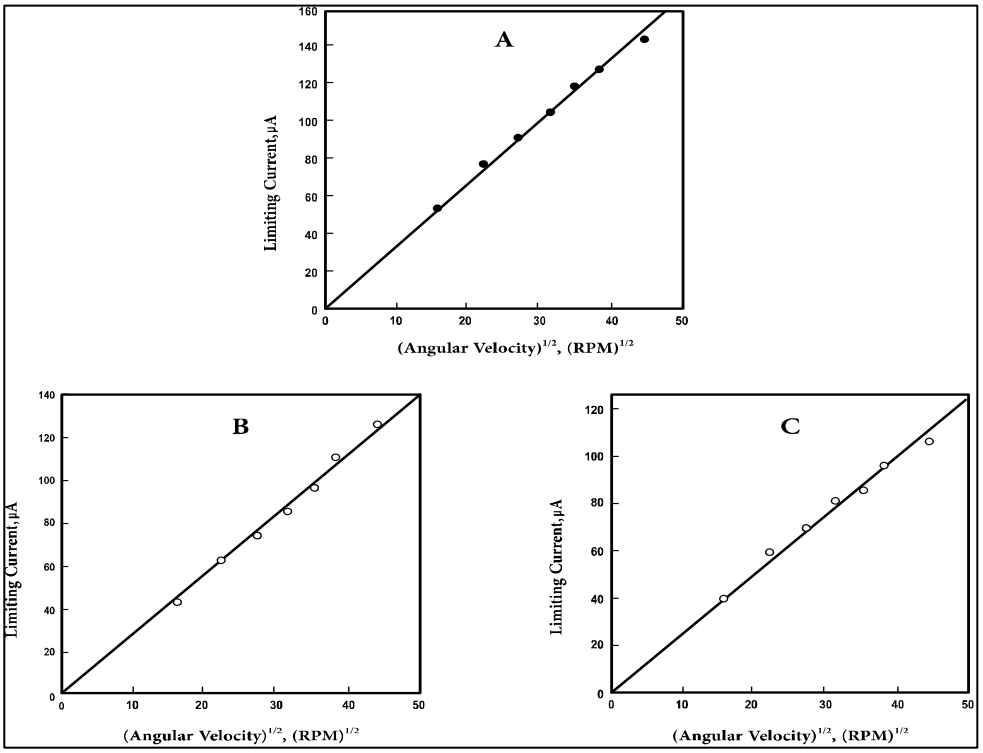

Figure 12. The plots of cathodic peak current (I_{pc}) versus the square root of angular velocity ($\omega^{1/2}$) in different media: A) Aqueous solution, B) EHSS micellar solution, C) EHSS microemulsion system.

3.3.3. Chronocoulometry

The chronocoulometric responses of 1,4-naphthoquinone were recorded in EHSS micelles and EHSS microemulsion systems as well as in pure aqueous solution by plotting the charge Q versus the time, t (Fig.13). The stepping time was 250 millisecond and the potential window was from 300 to –800 mV. The values of the amount of adsorbed reactant species, Γ_o are $2.13x^{-9}$, $2.15x10^{-9}$ and $4.29x10^{-9}$ $mole/cm^2$. An important aspect to be considered in electrochemical investigations in surfactant solutions is adsorption of the surfactant on the electrode surface and its effect on the electrochemical reactions. The previous electrochemical investigation of ferrocene in EHSS micelles and EHSS microemulsion did not show any significant effect that could be ascribed to surfactant adsorption on the electrode surface. All the results observed in this study could be explained based on electrostatic and hydrophobic interactions of the surface with the various species (reactant, intermediate & products) of the electrochemical reaction. However, in the absence of such interactions, the electrochemical behavior is not significantly affected.

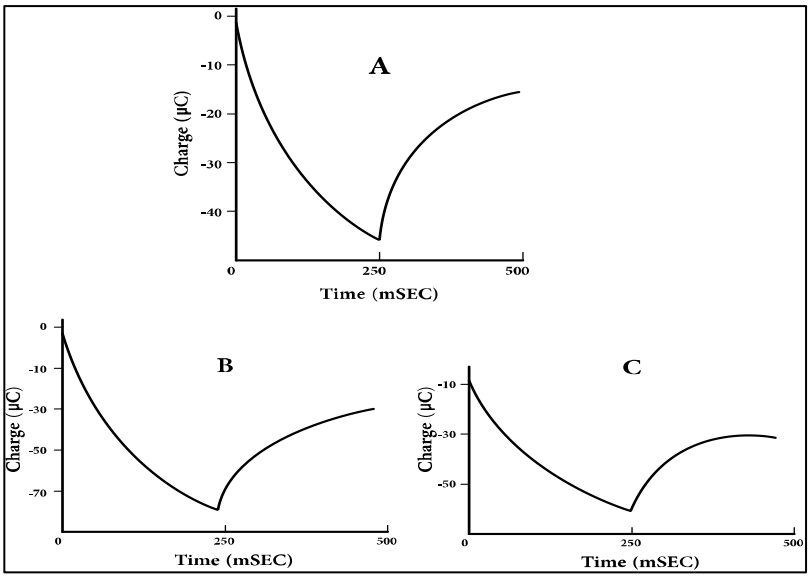

Figure 13. Chroncoulometric response of 1mM 1,4-naphthoqinone recorded in A) Aqueous solution, (B) EHSS micelle, (C) EHSS microemulsion system.

3.4. Electrochemical investigation of 2-methyl-1,4-Naphthoquinone (2-Me-1,4-NQ) in micelles and microemulsion media

3.4.1. Cyclic voltammetry

The cyclic voltammograms of 1 mM of 2-methyl-1,4-NQ in presence of 0.1 M NaCl as supporting electrolyte at different scan rates (20 – 500 mV/s) were recorded in EHSS micelles and microemulsion systems as well as in pure aqueous solution at the glassy carbon electrode, it is poorly soluble in water ($8.6x10^{-4}$ M) [40]. Its solubility is greatly enhanced by EHSS micelles and EHSS microemulsion. The voltammograms displayed one cathodic peak in the cathodic scan and one anodic peak in the reverse scan (Fig.14). The voltammograms in pure aqueous solution showed a similar voltammetric response, a single redox peak (Fig.16 A). The peak potential, ΔE_p, for aqueous solution is around 40 mV, whereas in EHSS micelles and EHSS microemulsion are around 156-159 and 113-119 mV, respectively (Table 8).

The data listed in Table (8) revealed that in EHSS microemulsion system, the ΔE_p increases slightly as the scan rate increases. Since the peak potential separation, ΔE_p, in completely reversible systems is equal to 59 mV for 1-electron transfer process and equals close to 30 mV for reversible 2-elcetron process and in the present study it is around 40, 107 and 115 mV in aqueous, EHSS micelles and EHSS microemulsion solutions, respectively (Table 11), thus, it is concluded that an electrochemical-chemical-electrochemical ECE) reaction occurs in these media in which protonation of the anion free radical generally leads to disprotonation reaction [38,39]. On the other hand, the ratio of I_{pa} / I_{pc} is less than unity and leads to 0.84, 0.74 and 0.84 at higher scan rates in aqueous, EHSS micelles and EHSS micelles, respectively (Table 8).

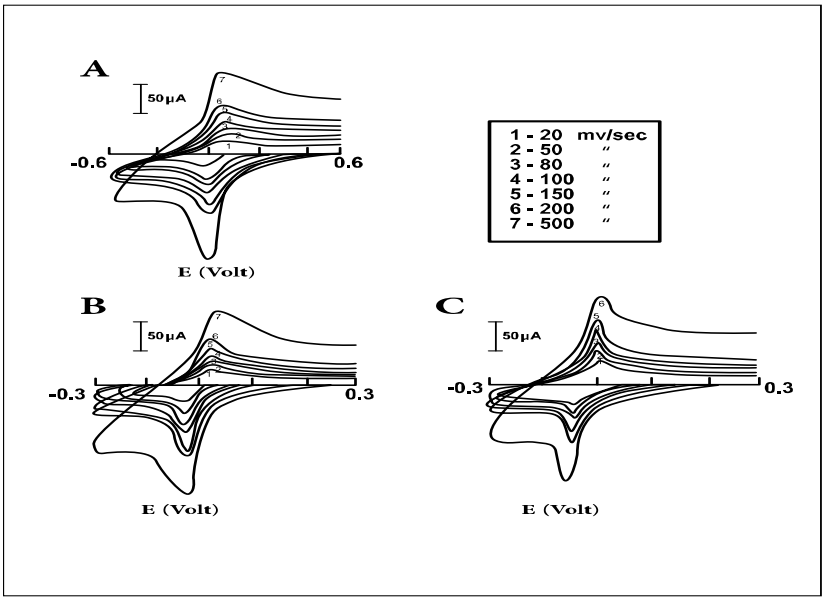

Figure 14. Cyclic voltammograms of $1x10^{-3}$ M 2-methyl-1,4-naphthoquinone recorded in A) Aqueous solution, B) EHSS micellar solution, C) EHSS microemulsion system.

Table 8. Cyclic voltammetric data obtained for 1 mM of 2-methyl-1,4-naphthoquinone in different systems.

Concentration	**Sweep rate, mV/ses**	**E_{pa} mV**	**E_{pc} mV**	**i_{pa} uA**	**i_{pa} uA**	**i_{pa}/i_{pc}**	**ΔE_p mV**
Pure aqueous	20	485	444	15.00	11.30	0.753	41
	50	486	444	27.50	20.00	0.727	42
	100	487	446	35.00	32.50	0.812	41
	200	488	445	57.50	57.50	0.826	43
	500	489	447	92.50	54.30	0.837	42
EHSS micelles	20	408	300	10.50	77.50	0.557	156
	50	408	301	17.50	11.87	0.640	156
	100	410	302	27.60	18.50	0.630	156
	200	410	304	39.89	25.90	0.680	159
	500	412	306	65.98	44.40	0.737	159
EHSS microemulsion	20	452	362	19.60	15.30	0.690	113
	50	452	362	30.20	24.70	0.757	114
	100	455	364	45.00	38.00	0.783	113
	200	457	363	60.85	2.30	0.865	116
	500	458	364	98.90	84.90	0.839	119

On employing the Randles-Sevcik equation, the plots of the anodic peak current, I_{pa}, and cathodic peak current, I_{pc}, versus the square root of sweep rate, $v^{1/2}$, in the different solutions, linear correlation deviated from the origin are shown (similar curves that as in Figure 10). From the slopes of these plots, the apparent diffusion coefficient values of the oxidized and reduced species, D^o_O and $D^o_{R,}$ were calculated and equal to $7.44x10^{-6}$, $4.46x10^{-6}$ and $4.8x10^{-6}$ cm^2/s for D^o_O and $9.79x10^{-6}$, $8.66x10^{-6}$ and $5.62x10^{-6}$ cm^2/s for D^o_R in aqueous, EHSS micelle and EHSS microemulsion solutions, respectively.

3.4.2. Rotating disk voltammetry

The rotating disk voltammograms (RDV) of 1 mM of 1-4-naphthquinone were recorded at small sweep rate (5 mV/s) in the potential window 800 to 1000 mV in pure aqueous solution as well as in EHSS micelles and EHSS microemulsion systems. The RDVs displayed single reduction wave in all media (Fig.15). It was found that, on increasing the rotation from 250 to 2000 RPM, a negative shift (~ 20mV) in the half-wave potential, $E_{1/2}$, indicating the chemical irreversibility which coincides with the greater ΔE_p values obtained from CV measurements. Logarithmic analysis of the RDVs were performed on plotting of log $(i/i_{L-}i)$ versus E in all investigated solutions which displayed parallel linear correlations at different rotation speed (250, 1000 & 2000 RPM) of slopes amounting to 23.2, 6.68 and 7.57 V for aqueous, EHSS micelles and EHSS microemulsion systems, respectively. These results indicate the quasi-reversible electron transfer process, since the calculated transfer coefficients (α) of the electro-reduction process in in the aqueous, EHSS micelles and EHSS microemulsion systems are 0.73, 0.59 and 0.45, respectively.

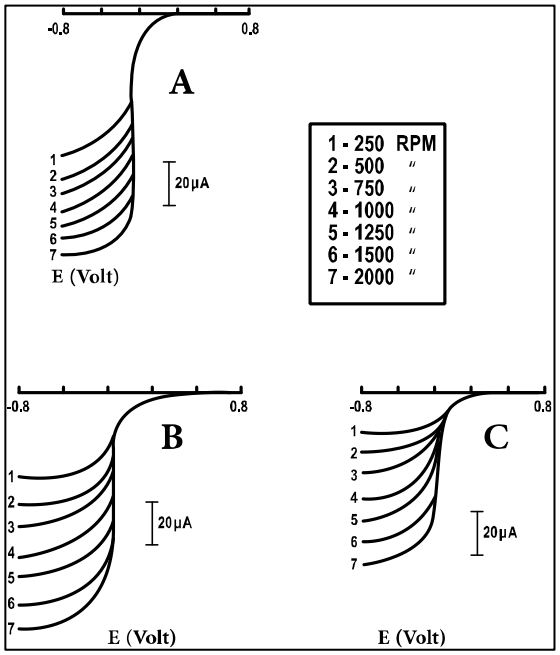

Figure 15. The effect of rotation speed of glassy carbon electrode on the linear sweep voltammograms obtained for 1mM in 2-methyl-1.4-naphthoquinone, (1) 250, (2) 500, (3) 750, (4)1000, (5) 1250, (6) 1500, (7) 2000 rpm, A) Aqueous solution, B) EHSS micellar solution, C) EHSS microemulsion system.

On using Levich equation, the plots of I_L versus $w^{1/2}$ in all media showed linear correlations (similar that as in Figure 12) passing through the origin, the behavior which indicates that the reduction process of 2-Me-1,4-NQ takes place under mass transfer control. From the slopes of these plots, the apparent diffusion coefficient values were calculated and found equal to $8.69x10^{-6}$, $6.32x10^{-6}$ and $5.34x10^{-6}$ cm^2/s in aqueous, EHSS micelle and EHSS microemulsion, respectively. The obtained results indicated the agreement of the D^o_R values calculated from cyclic voltammetry and those calculated from rotating disk voltammetry.

3.4.3. Chronocoulometry

The chronocoulometric responses of 2-methyl-1,4-naphthoquinone were recorded in EHSS micelles and EHSS microemulsion systems as well as in pure aqueous solution by plotting the charge Q versus the time, t (Fig.16). The stepping time was 250 millisecond and the potential window was from 300 to – 800 mV. The values of the amount of adsorbed reactant species, Γ^o are $2.61x^{-9}$, $1.02x10^{-8}$ and $4.00x10^{-9}$ mole/cm^2. An important aspect to be considered in electrochemical investigations in surfactant solutions is adsorption of the surfactant on the electrode surface and its effect on the electrochemical reactions. The previous electrochemical investigation of ferrocene in EHSS micelles and EHSS microemulsion did not show any significant effect that could be ascribed to surfactant adsorption on the electrode surface. All the results observed in this study could be explained based on electrostatic and hydrophobic interactions of the surface with the various species (reactant, intermediate & products) of the electrochemical reaction. However, in the absence of such interactions, the electrochemical behavior is not significantly affected.

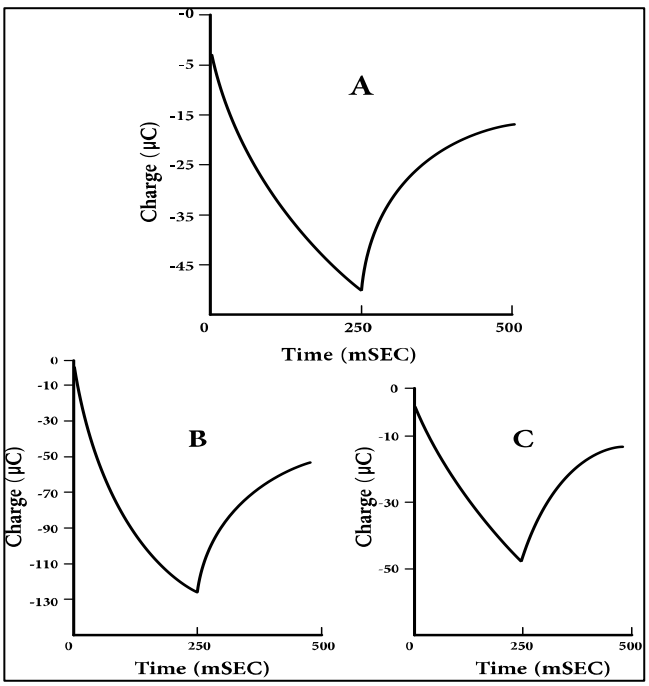

Figure 16. Chroncoulometric response of 1mM 2-methyl-1,4-naphthoqinone recorded in A) Aqueous solution, (B) EHSS micellar solution, (C) EHSS microemulsion system.

3.5. The electrode reaction mechanism

Cyclic voltammetric studies of 1,4-NAQ and 2-Me-1,4-NAQ in EHSS micelles and EHSS microemulsion systems as well as in pure aqueous solution displayed a single redox couple of two peaks observed on both the cathodic and anodic branches of sweep. The I_{pa}/I_{pc} ratio is less than unity in all media. The peak potential separation of both compounds, ΔE_p in is around 107 and 92 mV for 1,4-NAQ in micelles and microemulsion systems, respectively and around 157 and 115 mV for 2-Me-1,4-NAQ in micelles and microemulsion systems. On the other hand, ΔE_p in pure aqueous solution for both compounds is around 40 mV which is close to 30 mV, suggesting that electro-reduction of 1,4-NAQ and 2-Me-1,4-NAQ in pure aqueous solution is almost chemically reversible with a net transfer of two electrons. In other media such as EHSS micelles and EHSS microemulsion, ΔE_p increases to be 107 and 157 in micelles and 92 and 115 mV in microemulsion for the two naphthoquinone compounds, respectively. These results lead generally to the fact that an electrochemical-chemical-electrochemical (ECE) reaction nature in which protonation of the anion free radical generally leads to a disproportionation reaction. On the other hand, the rotating disk voltammograms of the two investigated compounds at different angular velocity showed a single reduction peak which exhibit cathodic shift of the $E_{1/2}$ with almost 20 mV on increasing the angular velocity. This behavior confirmed that the electrode reaction of these compounds takes place quasi-reversible in micelles and microemulsion systems. Chronocoulometry measurements in micelles and microemulsion system as well as in pure aqueous solution revealed that the values of amount of adsorbed reactant species at the electrode surface were found to be about 10^{-9} mole/cm^2 indicating a negligible adsorption at the electrode surface compared to the original solute concentration (1 mM).

In view of the obtained results, the electrode reaction mechanism of 1,4-NAQ and 2-methyl-1,4-NAQ at the glassy carbon electrode takes place via disproportionation reaction (equation 2.1) followed by the first electron transfer. Anionic surfactant and the substituent affect the disproportionation reaction to some extent. The proposed electrode reaction pathway of the two naphthoquinone compounds could take place as following:

a- 1,4-Naphthoqinone

$1,4\text{-NAQ} + e^- \leftrightarrow 1,4\text{-NAQ}^-$ … …… …	1
$1,4\text{-NAQ}^{-\cdot} + H^+ \leftrightarrow 1,4\text{-NAQH}^{\cdot}$ ……..	2
$2\,(1,4\text{-NAQ}^{-\cdot}) + 2H^+ \leftrightarrow 1,4\text{-NAQ} + 1,4\text{-NAQH}_2$ ……...	2.1
$1,4\text{-NAQH}^{\cdot} + e^- \leftrightarrow 1,4\text{-NAQH}^-$ …….	3
$1,4\text{-NAQH}^- + H^+ \leftrightarrow 1,4\text{-NAQH}_2$ ……	4

b- 2-Methyl-1,4-naphthoquinone

2-Methyl-1,4-NAQ + e^- ↔ 2-Methyl-1,4-NAQ$^-$ (1) …….	1
2-Methyl-1,4-NAQ$^{-\cdot}$ + H^+ ↔ 2-Methyl-1,4-NAQH$^{\cdot}$ ……	2
2 (2-Me-1,4-NAQH$^{\cdot}$) + $2H^+$ ↔ 2-Me-1,4-NAQ + 2-Me-NAQH$_2$	2.1
2-Me-1,4-NAQH$^{\cdot\cdot}$ + e^- ↔ 2-Me-1,4-NAQH$^-$ ……...	3
2-Me-1,4-NAQH$^-$ + H^+ ↔ 2-Me-1,4-NAQH$_2$ ……..	4

The above suggested mechanism agrees with those of analogous naphthoquinone derivatives in which the reduction processes occur via a two-electron quasi-reversible or completely reversible diffusion-controlled step. Several workers found that the electro-reduction of quinone compounds in aqueous buffer solutions of different pH values generating a single two-electron, two-proton step in acidic pH, while in alkaline pH the reduction does not involve protons and only a case of two-electron reduction step occurs. At neutral pH, the reduction is either one proton, two-electron step or two-electron without the participation of protons. The reduction process may be quasi-reversible or fully reversible depending on the pH value [43]. Dorn et al studied the electro-reduction of similar compounds, 2,3-diamion-1,4-napthoquinone and two of N-alkylated derivatives in acetonitrile using cyclic voltammetry. The cyclic voltammograms gave two reversible one-electron reduction waves. The peak potential separation is 64 ± 1 mV close to the value of fully one-reversible process [44]. Recently, the reduction of 1,4-naphthoquinone-amino acid and 2,3-dichloro-1,4-naphthoquinone was investigated using cyclic voltammetry. The voltammograms displayed one quasi-reversible, diffusion-controlled redox process in which the ratio i_{pa} / i_{pc} is close to one and proposed a reduction mechanism similar to our suggestion [45].

4. CONCLUSION

1-The Redox behavior of ferrocene in micellar and microemulsion media indicated a single one-electron fully reversible diffusion-controlled process, representing the oxidation of ferrocene to ferrocenim ion.

2-The voltammorams of both naphthoquinone compounds in micelle and microemulsion media display a single redox couple.

3- The redox reaction is two-electron quasi-reversible diffusion- controlled process, since the ratio i_{pa} / i_{pc} is slightly less than unity and ΔE_p is not close to the theoretical value of fully reversible process.

4- The rotating disk voltammograms display a cathodic shift as the angular velocity increases confirming that these results are in a good agreement with those of cyclic voltammetric data.

5- The diffusion coefficient values of both naphthoquinone compounds as well as ferrocene were determined using rotating disk electrode technique.

rr 6- The data of cyclic voltammetry and rotating disk electrode voltammetry revealed that the electrode reaction sequence of both naphthoquinone compounds is electrochemical-chemical electrochemical (ECE).

References

1. J. H. Flendles and E. J. Flendles, Catalysis in Micellar and Micromolecular Systems, Academic Press, New York, 1975.
2. P. Mukherjee*, J. Pharm. Sci.,* 63 (1979) 972.

3. R. Zana and R.A. Mackay, *Langmuir,* 2 (1986) 1242.
4. A. Berthed and J. Georges, *J. Coll. Inter. Sci.,* 106 (1985) 194.
5. G.L. Mcintire, D.M. Chupardy, R.L. Casselberry and H.N. Blount, *J. Phys. Chem.,* 86 (1982) 2632.
6. A. Berthed and J. Georgios, *J. Anal. Chim. Acta,* 147 (1982) 41.
7. E. Dayalan, S. Qutbuddin and A. Hussam, *Langmuir*, 6 (1990) 715.
8. K. R. Choksi, S. Qutbuddin and A. Hassan, *J. Coll. Inter. Sci*., 129 (1989) 315.
9. J. Texter, F.R. Hooch, S. Qutbuddin and E. Daylen, *J. Coll. Inter. Sci*., 135 (1990) 236.
10. E. Dayalan, S. Qutbuddin and J. Texter*, J. Coll. Inter. Sci*., 143 (1990) 423.
11. R.A. Mackay, S.A. Myers, L. Babubhai and A. Barter-Toth, *Anal. Chem*., 62 (1990) 1084.
12. N. G. Deniz, Z. G. Gunmen, M. Tsarevich, V. Novikov, O. Komarov ska- Porokhyavet, M. Ozyurek, K. Guru, D. Karaka and E. Ulukaya, *Chem. Pharm. Bull.*, 63 (2015) 1029.
13. P. A. J. Ferraz, F. C. de Abreu, A. V. Pinto, V. Glazer, T. Trenholm and M. O. F. Goulart, *J. Electroanal .Chem.,* 507 (2001) 275.
14. M. Gomeaz. F. J. Gonzalez and I. Gonzalez, *J. Electroanal. Chem.,*578 (2005)193.
15. M. Elharbi, P. Sid row, E. Cesar-Rodo, D. A. Lanfranch, E. Devious- Charset, D. Horvath and A. Vanek, *Chem. A .Europe. J.,* 21 (2015) 3415.
16. M. A. Haque, M. M. Rahman, M. A. B. H Susan*, J. Solution Chem*., 41 (2012) 447.
17. T. K Sen, A. Kambarka and J. B. Baruch, Dyes *Pigm.,* 75 (2007) 770.
18. E. H. G. *ola* Cruz, C. M. B. Mussée, G. G. Dias, E. B.T. Diogo, I. M.M. de Melo, B. L. Rodrigues, M. G. da Silva, W. O. Valencia, C. A. Camara, R. N. de Oliverira, Y. G. de Paiva, M. O. F. Goulart, B. C. Cavalant, C. Pessoa and E. N. de Silva Junior, *Bioorg. Med. Chem.*, 22 (2014) 1608.
19. M. A. H. M. Muhibbah Rahman and M. A. H. Susan, *J. Solution Chem*., 40 (2011) 861.
20. M. Quan, D. Sanchez, M. F. Waska and D. K. Smith, *J. Am. Chem. Soc.,* 129 (2007) 12847.
21. P. S. Guin, S. Das and P. C. Mandl, *Int. J. Electochem*., ID 816202, (2011) 1.
22. M. Abdallah, M. M. Al Faker, N. F. Hasan, M. A. Alharbi and E. M. Mabrouk, *Orient. J. Chem*., 35 (2019) 98.
23. E. M. Mabrouk, R. N. Felly and E. H. El- Mussallem, *Int. Electrochem. Sci*., 11 (2016) 4892.
24. O. A. Hazzai, R. El-Sayed and E. M. Mabrouk, *J. Adv. Chem.,* 7 (2014) 1271.
25. M. Von Stackelberg, M. Pilgrim and V.Z. Toome, *Electrochem*., 57 (1953) 342.
26. A. J. Adams, Electrochemistry at Solid Electrodes, Dekker, 1969.
27. A. J. Bard and L. R. Faulkner, Electrochemical Methods Fundamentals and Applications, Wiley, New York, 1980.
28. V. G. Leveche, Physicochemical Hydronamics, Prentice Hall, Englewood Cliffs, N.J.,1962.
29. N. S Neghmouche, A. Kelef and T. Lanes*, Rev. Sci. Found. App.,* 1 (2009) 23.
30. N. G. Tsierkezos, *J. Solution Chem.,* 36 (2007) 289.
31. G. Fenny and Y. Yang, *Electrochim. Acta,* 53 (2008) 8235.
32. P. Zaninelli and G. Giorgi, *Inorg. Chim. Acta,* 255 (1997) 47.
33. P. Zaninelli and N. D. Rauch , *J. Organometallic Chem*., 471 (1994) 1.
34. J. Georgios and S. Demetra, *Electrochim. Acta.*, 29 (1984) 521.
35. J. Georgios and A.J. Berthed, *J. Electroanal. Chem.,* 143 (1984) 175.
36. F. C. Anson, *Anal. Chem.,* 38 (1966) 54.
37. F. C. Anson, J. H. Christie and R. A. Oster young, *J. Electroanal. Chem.,*13 (1967) 234.
38. D. Hawley, S. W. Feldberg*, J. Phys. Chem.,* 70 (1966) 3459.
39. C. Amatory and J. M. Save at, *J. Electroanal. Chem.,* 107 (1980) 353.
40. A. Berthed, R. A. Mackay and J. Texter, Electrochemistry in Colloids and Dispersions, Ed., VCH Publishers, Inc., New York, 1992.
41. D. Hawley and S. W. Feldberg, *J. Phys. Chem*. 70 (1966) 3459.
42. C. Amatore and J. M. Savant, *J. Electroanal. Chem*., 107 (1980) 353.
43. P. S. Guinn, S. Das, P. C. Mandal, *Int. J. Electrochem. Sci.,* 291 (2011) xxx.
44. P. I. Dorn, S. Romanova, N. P. Halloran, L. Pospisil and J. Michl*, Electroanalysis,* 28 (2016) 2855.

45. E. Rivera-Avalos, D. de Louera, J. G. Araujo-Huit ado, I. L. Escalant-Garcia, M. A. Munoz-Sanchez, H. Hernandies, J. A. Lopez and L. Lopez, *Molécules*, 24 (2019) 4285.